

Evaluating Synthesized Schiff base as Corrosion Inhibitor on Carbon Steel in 0.5 M HCl and 0.5 M H₂SO₄

B. A. Elsayed, M. A. Hegazy, H. M. H. Abd El-Bary, Ahmed A. Abdel Salam

Abstract: The inhibition effect of synthesized schiff base on the corrosion of carbon steel in (0.5 M HCl and 0.5 M H₂SO₄) was studied at different temperatures (25–55 °C) by weight loss, electrochemical impedance spectroscopy (EIS) and potentiodynamic polarization methods. The carbon steel surface morphology was investigated by SEM. The obtained results showed that the prepared schiff base is excellent inhibitor in (0.5 M HCl and 0.5 M H₂SO₄) and the inhibition efficiency (η) increases with the inhibitor concentration, but it decreases with increasing temperature. The adsorption of inhibitor on the surface of carbon steel is mixed chemical and physical adsorption and found to obey the Langmuir adsorption isotherm equation. Thermodynamic parameters have been obtained by adsorption theory. Polarization curves showed that the synthesized inhibitor is mixed-type inhibitor in both hydrochloric acid and sulfuric acid. Data obtained from electrochemical impedance spectroscopy (EIS) studies were analyzed to model-inhibition process through appropriate equivalent circuit model. Potentiodynamic polarization studies have been shown that the inhibitor acts as a mixed type of inhibitor. Scanning electron microscope (SEM) confirmed the protection of the carbon steel surface by the inhibitor.

Keywords: (0.5 M HCl and 0.5 M H₂SO₄), (EIS), SEM., (25–55 °C), (η), (EIS), Potentiodynamic, hydrochloric

I. INTRODUCTION

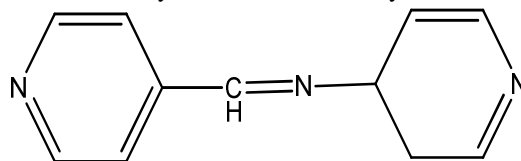
Carbon steel is mainly used in many applications, including the construction of bridges, mega factories, drilling machinery, tanks and pipelines production and petroleum refining. The use of hydrochloric acid in pickling of metals, acidization of Oil wells and cleaning of scales is more economical, efficient and Trouble-free, than other mineral acids¹. Inhibitors are used to prevent metal dissolution as well as acid consumption. The most well-known acid inhibitors are organic compounds containing nitrogen, phosphor, sulfur, and oxygen atoms. Acid solutions are generally used in several industrial processes. In acidic media, corrosion inhibitor is the most practical methods to protect the metal surface from acidic effect. A review dealing with various types of organic inhibitors has been previously published. Compounds containing functional groups with heteroatoms,

Which can donate lone pair electrons, are found to be very efficient as inhibitors against metal corrosion in many environments. Many N-heterocyclic compounds with polar groups and/or electrons are efficient corrosion inhibitors in acidic solutions. Organic molecules of this type can adsorb on the metal surface and form a bond between the N-electron pair and/or the electron cloud and the metal, thereby reducing the corrosion in acidic solutions². Most of the commercial inhibitor formulations consist of amines. Due to the presence of the (–C=N–) group in the molecule, Schiff bases represent as good corrosion inhibitors. Some researches revealed that the corrosion inhibition efficiency of the Schiff bases is better than the corresponding amines and aldehydes³. The Schiff base has been previously reported as an effective corrosion inhibitor for steel, copper and aluminum^{4,5}. The adsorbed species protect the metal from the aggressive medium, which causes decomposition of the metal. Adsorption process depends on not only the nature and the charge of the metal but also on the chemical structure of the inhibitor. The aim of the present investigation was to examine the corrosion Inhibition effect of Schiff base (N-(pyridine-4-ymethylene)-3,4-dihydropyridine-4-amine) for carbon steel in (0.5M HCl and 0.5M H₂SO₄).

II. MATERIALS AND EXPERIMENTAL TECHNIQUES

2.1. Synthesis of Schiff base compound

Schiff base compound used in this study was synthesized through Schiff base reaction⁶ between (0.1 mol, 10.7 g) of 4-nicotine aldehyde and (0.1 mol, 9.4 g) 4-aminopyridine to produce (N-(pyridine-4-ymethylene)-3, 4-dihydropyridine-4-amine). The reaction mixture was refluxed for 4h in 70 °C the product was evaporated from acetone to produce The chemical structure of the synthesized inhibitor (Fig. 1).the Schiff base was confirmed by FTIR, mass and 1H NMR spectroscopy. FTIR analysis was carried out using ATI mattsonm Infinity series TM, Bench top 961 controlled by Win First TM V2.01 software .1H NMR was measured in CDC13 using Jeol ECA 500 MHz NMR spectrometer, at 500 mHz. Mass analysis was carried out by GC MS-OP1000EX.



N-(pyridin-4-ylmethylene)-3,4-dihydropyridin-4-amine
Fig1 the chemical structure of the synthesized inhibitor.

Revised Version Manuscript Received on June 24, 2016.

Prof. Badr A. El-sayed, Department of Chemistry, Faculty of Science, Al-Azhar University, Nasr City, Cairo, Egypt.

Prof. M. A. Hegazy, Department of Physical Chemistry, Egyptian petroleum research, Cairo, Egypt.

Prof. H. M. H. Abd El-Bary, Department of Chemistry, Faculty of Science, Al-Azhar University, Nasr City, Cairo, Egypt.

Ahmed A. Abdel Salam Department of Chemistry, Faculty of Science, Al-Azhar University, Nasr City, Cairo, Egypt.

2.2. Solutions

The aggressive solutions, 0.5 M HCl and 0.5 M H₂SO₄, were prepared by dilution of analytical grade 37% HCl with distilled water and 98% H₂SO₄ with distilled respectively. The concentration range of synthesized inhibitors varied from 1×10⁻³ to 1×10⁻² M.

2.3. Carbon steel

Tests were performed on carbon steel of the following composition (wt.%): 0.19% C, 0.05% Si, 0.94% Mn, 0.009% P, 0.004% S, 0.014% Ni, 0.009% Cr, 0.034% Al, 0.016% V, 0.003% Ti, 0.022% Cu, and the rest is Fe.

2.4. Electrochemical measurements

The electrochemical experiments were carried out in a conventional three-electrode cell with a platinum counter electrode (CE) as auxiliary electrode and silver/silver chloride (Ag/Ag) as a reference electrode. A working electrode (WE) was a rod of carbon steel embedded in PVC holder using epoxy resin so that the flat surface was the only exposed surface in the electrode. The exposure surface area of the working electrode was 0.8 cm². This area was abraded with emery paper (grade 320, 400, 600, 800, 1000, 1200) on the test face, rinsed with distilled water, degreased with acetone, and then dried. Before measurement, the electrode was immersed in a test solution at open circuit potential (OCP) for 30 min until a steady state was reached. All Electrochemical measurements were recorded by a Volta lab 40 Potentiostat PGZ 301. Each experiment was repeated three times to check the reproducibility. Electrochemical impedance spectroscopy (EIS) measurements were carried out as described before ⁷. A small alternating Voltage perturbation (5 mV) was imposed on the cell over the frequency Range of 100 kHz to 30 mHz at open circuit potential at 20 °C.

2.4.1. The inhibition efficiency (η_I)

The corrosion inhibition efficiency (η) was calculated from the values of (R_{ct}) using the following equation ⁸:

$$\eta_I = \left(\frac{R_{ct}^o - R_{ct}}{R_{ct}^o} \right) \times 100 \dots \dots \dots (1)$$

Where (R_{ct}^o) and (R_{ct}) are the charge transfer resistance values in the presence and absence of the inhibitor, respectively.

2.4.2. The double layer capacitance (C_{dl})

The double layer capacitance (C_{dl}) was calculated from the following equation ⁹:

$$C_{dl} = \gamma^o (\omega_{max})^{n-1} \dots \dots \dots (2)$$

Simplified to

$$C_{dl} = \frac{1}{2\pi R_{ct} f_{max}} \dots \dots \dots (3)$$

Where f_{max} is the frequency at maximum imaginary component of the impedance. The Helmholtz model equation ¹⁰:

$$\delta_{org} = \frac{\epsilon \epsilon_0 A}{C_{dl}} \dots \dots \dots (4)$$

Where ε dielectric constant of the medium is, ε₀ is the vacuum Permittivity, A is the electrode surface area, and

δ_{org} is the thickness of the protective layer. Potentiodynamic polarization measurements were obtained by changing the electrode potential automatically from -750 to -300 mV vs. Ag/Ag with scan rate 2 mV s⁻¹ at 20 °C.

2.4.3. The inhibition efficiency (η_p)

The corrosion inhibition efficiency (η_p) was calculated using the following equation ¹⁰:

$$\eta_p = \left(\frac{i_{corr} - i_{corr}^o}{i_{corr}} \right) \times 100 \dots \dots \dots (5)$$

Where i_{corr}, i_{corr}^o is corrosion current density in presence and absence of inhibitor, respectively, which determined by extrapolation of the cathodic and anodic Tafel lines to the respective free corrosion potential.

2.5. Weight loss measurements

Carbon steel sheets of 5.92 × 2.43 × 0.38 cm were abraded with a series of emery paper (grade 320–400–600–800–1000–1200) and finally washed with distilled water and acetone. After accurately weighted, the specimens were immersed in a closed beaker containing 130 ml of 0.5 M HCl and another closed beaker containing 0.5 M H₂SO₄ with and without different concentrations of synthesized inhibitor. The steel specimens were taken out after 24 h. Then they were rinsed with distilled water two times and degreased with acetone. Afterword the specimens were immersed in 0.5 M HCl solution for 10 sec. (chemical method for cleaning rust products), rinsed twice with distilled water, dried, and accurately weighted. The experiments were carried out in triplicates to get good reproducibility. The average weight loss of three parallel carbon steel sheets was obtained. Immersion time of weight loss is 24 h at all studied temperatures.

2.5.1. The corrosion rate (k)

The value of corrosion rate (k) was calculated from the following equation ¹¹:

$$k = \frac{\Delta W}{St} \dots \dots \dots (6)$$

Where ΔW = W_o - W_s is the average weight loss of three parallel carbon steel, W_o Blank weight specimen before immersion, W_s Sample weight specimen after immersion, S is the total area of the Sheet and t is the immersion time 24 h.

2.5.2. The corrosion inhibition efficiency (η_w)

The corrosion inhibition efficiency (η_w) of carbon steel was calculated

From the following equation ¹²:

$$\eta_w \% = \left(\frac{w_{corr} - w_{corr}^o}{w_{corr}} \right) \times 100 \dots \dots \dots (7)$$

Where w_{corr} and w_{corr}^o are the weight loss of carbon steel in the absence and presence of the inhibitor, respectively.

2.5.3. Langmuir isotherm

The simplest isotherm equation is Langmuir ¹³:

$$\frac{C}{\theta} = \frac{1}{K_{ads}} + C \dots \dots \dots (8)$$



Where K_{ads} the binding constant of the adsorption reaction, C is the inhibitor concentration in the bulk phase of the solution, and θ is the surface coverage.

2.5.4. The degree of surface coverage (θ)

The degree of surface coverage (θ) for different concentrations of inhibitor molecules in 0.5 M HCl and 0.5 M H₂SO₄ respectively was calculated from weight loss measurements using the following equation:

$$\theta = \left(\frac{W - W_0}{W} \right) \dots \dots \dots (9)$$

Where W_0 and W are the values of the weight loss with and without addition of the inhibitor, respectively.

2.5.5. The standard free energy (ΔG°_{ads})

The standard free energy (ΔG°_{ads}) was obtained according to the following equation¹⁴:

$$\Delta G^\circ_{ads} = -RT \ln(55.5 K_{ads}) \dots \dots \dots (10)$$

Where the value 55.5 is the concentration of water in solution expressed in (M).

2.5.6. The standard enthalpy (ΔH°_{ads})

The standard enthalpy, (ΔH°_{ads}), was calculated according to the

Van't Hoff equation¹⁵:

$$\ln K_{ads} = - \left(\frac{\Delta H^\circ_{ads}}{RT} \right) + constant \dots \dots \dots (11)$$

Where (ΔH°_{ads}) and K_{ads} are the standard enthalpy and adsorptive equilibrium constant, respectively.

2.5.7. The standard entropy (ΔS°_{ads})

According to the thermodynamic basic equation, the standard entropy, (ΔS°_{ads}), was calculated from the following equation¹⁶:

$$\Delta G^\circ_{ads} = \Delta H^\circ_{ads} - T\Delta S^\circ_{ads} \dots \dots \dots (12)$$

2.5.8. Apparent activation energy (E_a)

Apparent activation energy (E_a) of the steel in acidic media was calculated from the natural logarithm of the corrosion rate k in (gm⁻² h⁻¹) which is a linear function with 1/T (following Arrhenius equation)¹⁷:

$$K = Ae^{-\frac{E_a}{RT}} \dots \dots \dots (13)$$

Simplified to

$$\ln K = -\frac{E_a}{RT} + \ln A \dots \dots \dots (13)$$

Where E_a and A represent the apparent activation energy and the pre-exponential factor, respectively.

2.5.9. Enthalpy and entropy of activation (ΔH° and ΔS°)

Enthalpy and entropy of activation (ΔH° and ΔS°) were calculated from the transition state theory¹⁸:

$$\ln \left(\frac{K}{T} \right) = \left(\ln \left(\frac{R}{N_A h} \right) + \left(\frac{\Delta S^\circ}{R} \right) \right) - \frac{\Delta H^\circ}{RT} \dots \dots \dots (14)$$

Where h is the Planck's constant, N_A is the Avogadro's number, R is the universal gas constant, ΔH° is the enthalpy of the activation and ΔS° is the entropy of activation.

2.6. Scanning electron microscope (SEM)

The carbon steel specimens of size (5.92 cm - 2.43 cm - 0.38 cm) were abraded with Abrasive paper (grade 320-400-600-800-1000-1200) to remove protective layer. Then washed with distilled water and acetone for (0.5 M hydrochloric acid, 0.5 M sulfuric acid) without and with addition of (1×10^{-2}) of the prepared (SB) at room temperature 25 °C for 24 h, take the specimens away of corrosive media cleaned with distilled water, dried with a cold air, and then applied the test with SEM Jeol JSM-5400.

III. RESULTS AND DISCUSSION

3.1. Characterization of the structure of synthesized inhibitor

Structure of the synthesized inhibitor has been characterized as previous¹⁹ by FTIR, ¹H NMR, and mass spectral analysis.

3.2. Electrochemical impedance spectroscopy (EIS)

The corrosion behavior of carbon steel in both (0.5 M HCl and 0.5 M H₂SO₄ respectively) in the presence and absence of the synthesized inhibitor was investigated using EIS at 20 °C. Nyquist plots of carbon steel in both (0.5 M HCl and 0.5 M H₂SO₄ respectively) solutions without and with various concentrations of inhibitor Schiff base are shown in Figs 2(a, b) respectively. The Nyquist plots (Figs.2 (a, b) showed perfect semicircles as expected from the theory of EIS. The Nyquist plots obtained in the real system represent a general behavior where the double layer on the interface of metal/solution does not behave as a real capacitor. On the metal side, electrons control the charge distribution whereas on the solution side it is controlled by ions. As ions are much larger than the electrons, the equivalent ions to the charge on the metal will occupy quite a large volume on the solution side of the double layer. Therefore, the constant phase element (CPE) used in place of double layer capacitance at the metal substrate/solution interface C_{dl} , to represent the non-ideal capacitive behavior of the double layer. EIS spectra of the synthesized inhibitor were analyzed using the equivalent circuit in Fig. 3. It represented a single charge transfer reaction and it fitted well with our experimental results. The intersection of the capacitive loop with the real axis represented the ohmic resistances of the corrosion product films and the solution enclosed between the working electrode and the reference electrode, R_s ²⁰. R_{ct} represented the charge transfer resistance and its value was a measure of electron transfer across the surface and was inversely proportional to the corrosion rate²¹. Results listed in Table 1 showed that the charge transfer resistance, R_{ct} , values increased and the capacitance values C_{dl} decreased with increasing inhibitor concentration in both of (0.5 M HCl and 0.5 M H₂SO₄) respectively. Decreasing in the capacitance, which can result from a decrease in local dielectric constant and/or an increase in the thickness of the electrical double layer, suggested that the inhibitor molecule acted by adsorption at the metal/solution interface. The addition of the synthesized inhibitor resulted in lower, C_{dl} , values 0.5 M HCl and lower dramatically in 0.5 M H₂SO₄, which could be a consequence of the replacement of water molecule by inhibitor molecule at the



electrode surface. The inhibitor molecule may also reduce the capacitance by increasing the double layer thickness according to the Helmholtz model Eq. (4). So the value of C_{dl} became smaller in the presence of the inhibitor than in its absence. Due to the effective adsorption of the synthesized inhibitor²². For expiation more complicated system of inhibition, Bode plots can give more information. Bode plots refer to representation of the impedance magnitude (or the real or imaginary components of the impedance) and phase angle as a function of frequency. The Bode plots of the synthesized inhibitor schiff base are shown in Figs. 4(a, b). The low frequency impedance modulus Z_{mod} is one of the parameters which can be easily used to compare corrosion resistance of the inhibitor in different concentration of used corrosive media. Increasing in Z_{mod} demonstrates better protection performance as reported before²³. Fig. 4(a, b) showed that Z_{mod} increases as a function of the concentration for the synthesized inhibitor. The explanation of these result can be attributed to many frequency range, the high frequency phase angle range (10^5 – 10^4 Hz) of the impedance spectra which represents the properties of an outer layer, the middle frequency range (10^4 – 10^2 Hz) reflects the properties of an inner barrier layer, while the low frequency range (less than 10^2 Hz) relates to the properties of the double–electrical layer information²⁴. Therefore, the high frequency

phenomenon is due to increasing in the thickness of the outer porous layer, and the middle frequency phenomenon can be attributed to the penetration of active chloride ions and water through the defect of the synthesized inhibitor inner barrier layer, though the whole effect induced the increase of Z_{mod} . As seen from Fig.4 (a, b) Bode plots refer to the existence of an equivalent circuit that contains a single constant phase element in the metal/solution interface. The increase of absolute impedance at low frequencies in Bode plots confirmed the higher protection with increasing the concentration of the inhibitor, which is related to adsorption of the inhibitor on the carbon steel surface²⁵. The phase angle plots for the carbon steel in the presence and absence various inhibitor concentrations in both (0.5 M HCl and 0.5 M H₂SO₄) solutions are given in Fig. 4(a, b). According to the appearance of phase angle plots, increasing the concentration of the inhibitor enhanced the superior inhibitive behavior due to increasing adsorption of the more inhibitor molecule on the metal surface. Furthermore, the depression of phase angle at relaxation frequency occurs with decreasing of inhibitor concentrations which indicated the decrease of capacitive response with the decrease of inhibitor concentration. Such a phenomenon could be attributed to higher corrosion activity at low concentration of inhibitor.

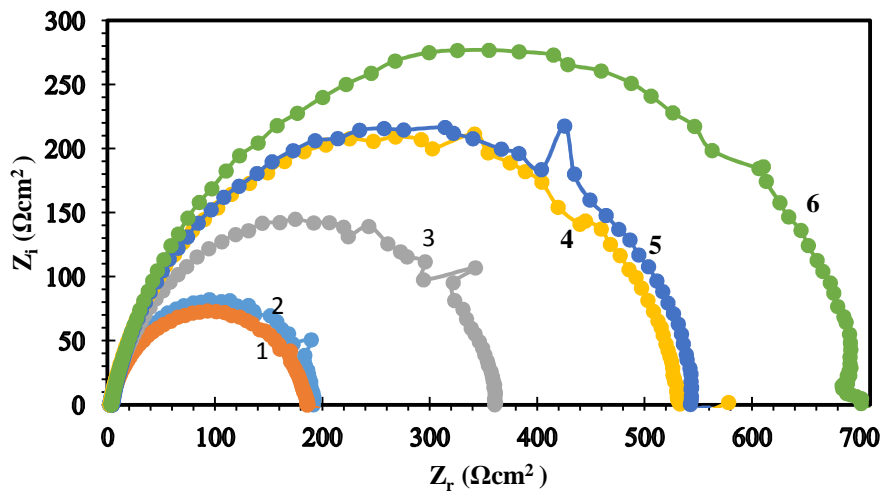


Fig .2 a. Nyquist plots for carbon steel in 0.5 M HCl in absence and presence of different concentrations of S.B. (1) 0.5 M HCl, (2) 1×10^{-3} M, (3) 2.5×10^{-3} M, (4) 5×10^{-3} M, (5) 7.5×10^{-3} M, and (6) 1×10^{-2} M.

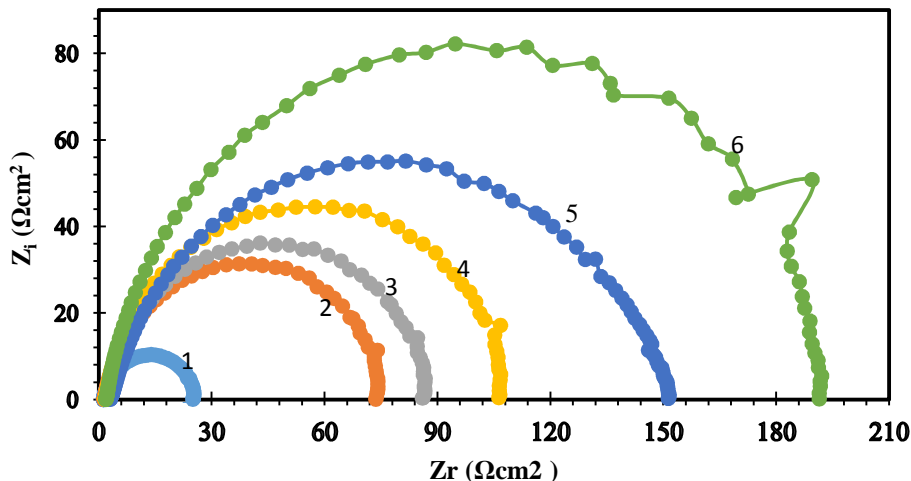


Fig .2b. Nyquist plots for carbon steel in 0.5 M H₂SO₄ in absence and presence of different concentrations of Schiff Base. (1) 0.5 M H₂SO₄, (2) 1×10^{-3} M, (3) 2.5×10^{-3} M, (4) 5×10^{-3} M, (5) 7.5×10^{-3} M, and (6) 1×10^{-2} M.

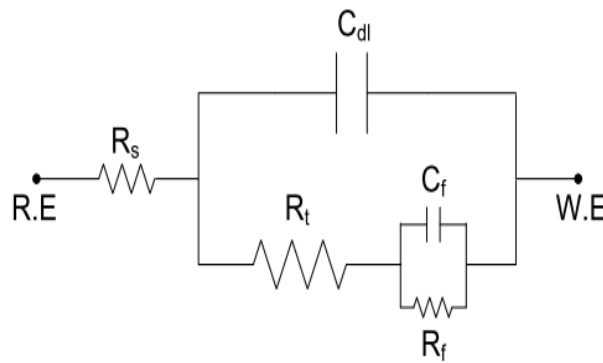


Fig 3 the suggested equivalent circuit model for the studied system.

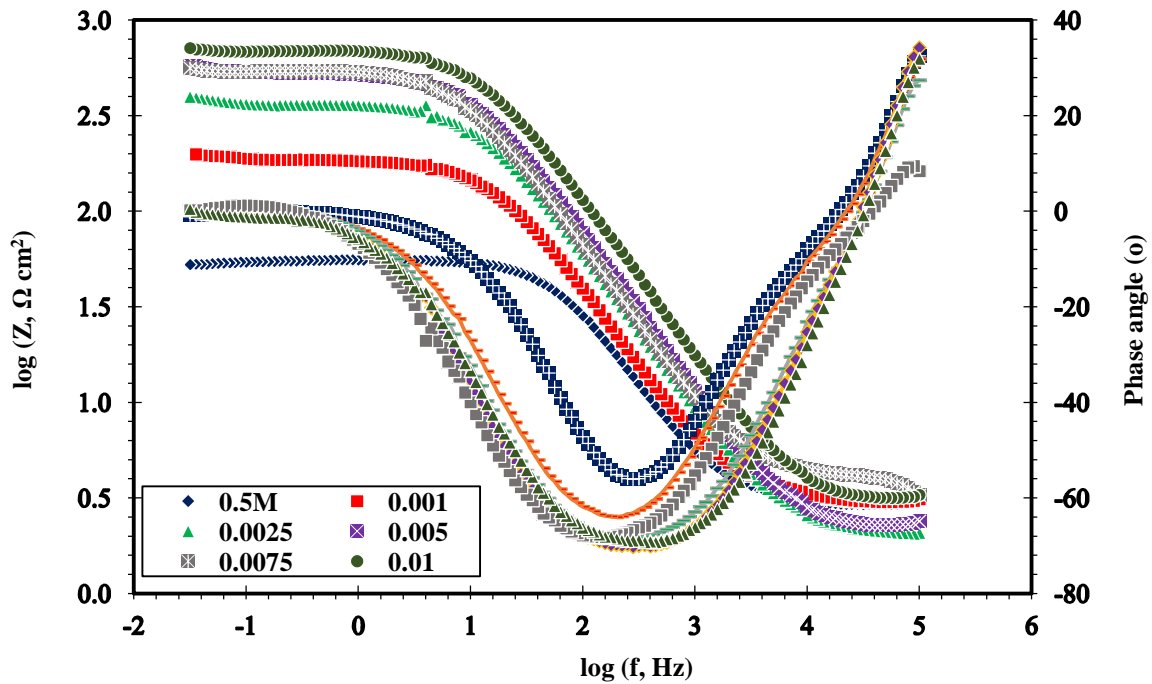


Fig 4a Bode and phase angle plots for carbon steel in 0.5M HCl in the absence and presence of different concentrations of Schiff base.

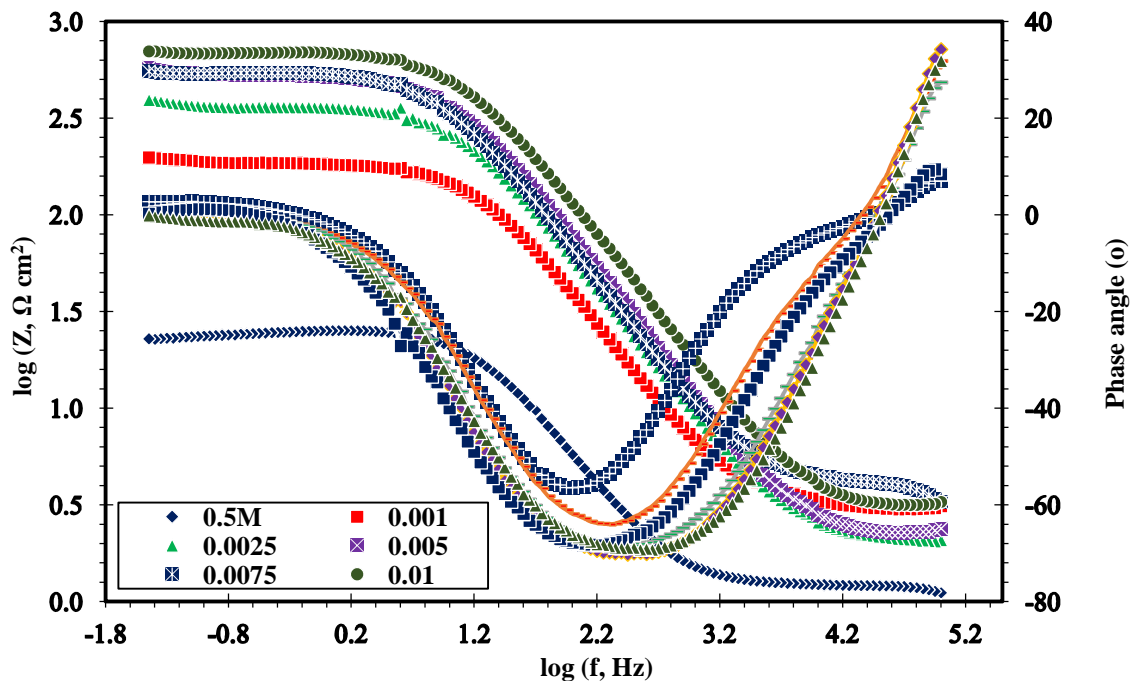


Fig 4 b Bode and phase angle plots for carbon steel in 0.5M H₂SO₄ in the absence and presence of different concentrations of Schiff base.

Table 1. EIS parameters for the corrosion of carbon steel in both (0.5 M HCl and H₂SO₄) in absence and presence of different concentrations of the prepared Schiff base at 20 °C.

Acid name	Conc of Inhibitor (M)	R _s (ohm cm ²)	R _{ct} (ohm cm ²)	C _{dl} (μ F cm ⁻²)	η _i (%)
0.5 M HCl	0.00	3.057	52.94	53.50	
	1×10 ⁻³	3.069	182.8	48.74	71.70932358
	2.5×10 ⁻³	2.670	360.0	31.47	80.28641073
	5×10 ⁻³	2.097	531.9	26.8	86.94393662
	7.5×10 ⁻³	2.72	601.3	21.3	90.46313224
	1×10 ⁻²	3.949	694.0	18.34	93.93662401
0.5 M H ₂ SO ₄	0.00	1.217	24.51	363.5	
	1×10 ⁻³	1.488	74.12	76.44	68.39647577
	2.5×10 ⁻³	1.831	86.02	65.86	72.18502203
	5×10 ⁻³	1.793	106.3	59.88	78.7753304
	7.5×10 ⁻³	2.877	148.1	53.71	83.33920705
	1×10 ⁻²	2.165	191.7	46.48	88.03524229

3.3. Potentiodynamic polarization

The polarization behavior of carbon steel in in both (0.5 M HCl and 0.5 M H₂SO₄) in the presence and absence of different concentrations of inhibitor Schiff base at 20 °C is represented in Fig. 5(a, b). The corrosion current density (i_{corr}), corrosion potential (E_{corr}), cathodic Tafel slope (β_C), and anodic Tafel slope (β_A) values as functions of the synthesized inhibitor concentration, were calculated from the Tafel plots of the synthesized inhibitor and listed in Table 2. (β_A and β_C) values did not show significantly changes, this result indicated that the anodic and cathodic corrosion reaction mechanism did not change. The presence of the synthesized inhibitor slightly shifted the corrosion

potential (E_{corr}) to both negative and positive directions. This indicated that the synthesized inhibitor acted as a mixed type inhibitor²⁶. The inhibition efficiency values (η_p) obtained for the studied synthesized inhibitor are given in Table 2. The results showed that, i_{corr} decreased whereas η_p increased with increasing the inhibitor concentration. This can be related to the adsorption of the inhibitor over the cathodic and anodic active corroded surface. Increasing in corrosion inhibition efficiency of the studied inhibitor in case of 0.5 M HCl solution than that in 0.5 M H₂SO₄ Table2 indicated that the synthesized inhibitor had good inhibitive properties of the metal surface in HCl than H₂SO₄ solutions.

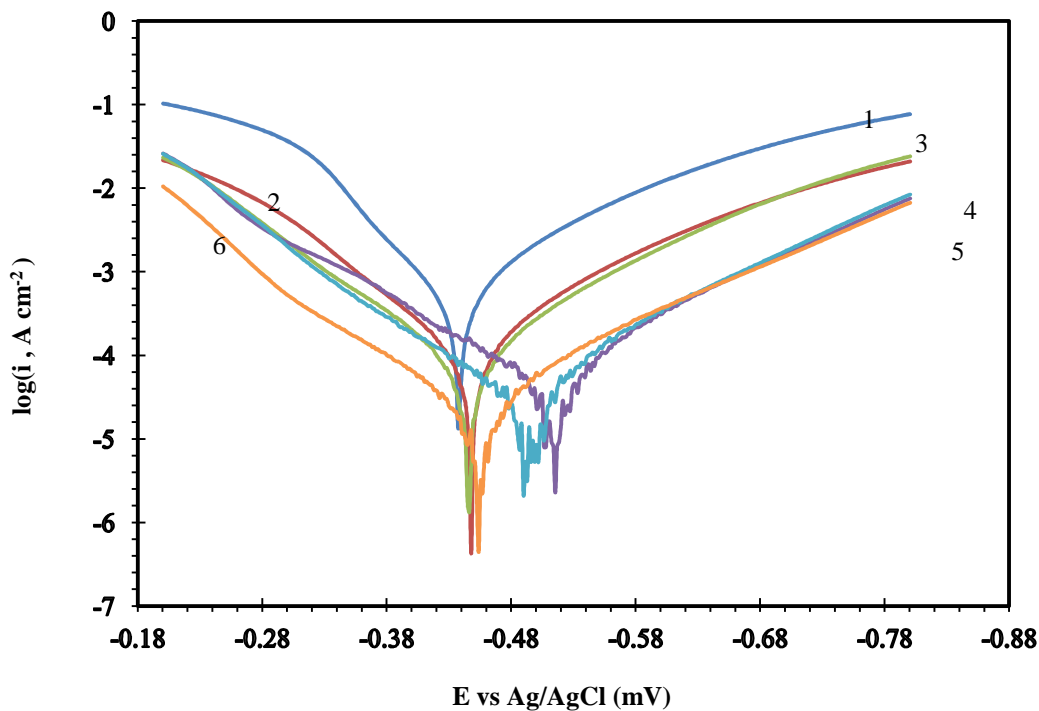


Fig.5.a Tafel curves obtained at 20 °C in 0.5 M HCl in absence and presence of different concentrations of Schiff Base. (1) 0.5 M HCl, (2) 1×10⁻³ M, (3) 2.5×10⁻³ M, (4) 5×10⁻³ M, (5) 7.5×10⁻³ M, and (6) 1×10⁻² M.

Table 2. Potentiodynamic polarization parameters for the corrosion of carbon steel in in both (0.5 M HCl and 0.5 M H₂SO₄) in absence and presence of different concentrations of the prepared Schiff base at 20 °C.

Type of corrosive solution	Conc of inhibitor (M)	-E _{Corr} (mV)	i _{Corr} (mA cm ⁻²)	β _a (mVdec ⁻¹)	-β _c (mVdec ⁻¹)	RP (Ωcm ²)	θ	IE. (%)
0.5 M HCl	Blank	450	0.6674	110.1	144.5	52.94	—	—
	1×10 ⁻³	450.4	0.2034	110.1	144.5	182.8	0.71709	71.7
	2.5×10 ⁻³	448.3	0.1377	110.9	135.2	360.0	0.80286	80.28
	5×10 ⁻³	517.5	0.0995	160.5	152.8	531.0	0.86943	86.94
	7.5×10 ⁻³	498.3	0.0697	135.7	145.8	595.0	0.90463	90.46
	1×10 ⁻²	457.5	0.0449	152	159.4	694.0	0.93936	93.93
0.5 M H ₂ SO ₄	Blank	440.5	1.1381	89.7	159.5	24.51	—	—
	1×10 ⁻³	435.0	0.3756	71.4	146.4	74.12	0.68396	68.39
	2.5×10 ⁻³	428.4	0.3279	70.7	155.9	86.02	0.73656	73.65
	5×10 ⁻³	442.4	0.2648	74.8	142.3	106.3	0.78775	78.77
	7.5×10 ⁻³	421.8	0.1952	69.0	152.9	148.1	0.83339	83.33
	1×10 ⁻²	440.1	0.1482	72.6	145.0	191.7	0.88035	88.03

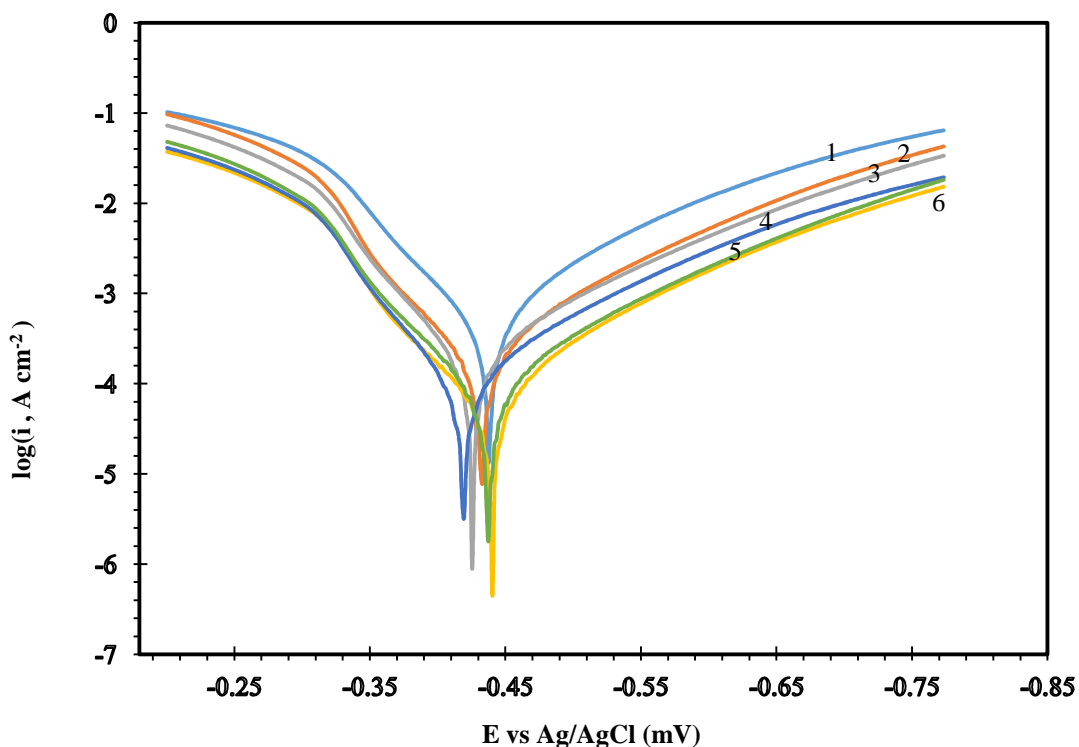


Fig5.b Tafel curves obtained at 20 °C in 0.5 M H₂SO₄ in absence and presence of different concentrations of Schiff Base. (1) 0.5 M H₂SO₄, (2) 1×10⁻³ M, (3) 2.5×10⁻³ M, (4) 5×10⁻³ M, (5) 7.5×10⁻³ M, and (6) 1×10⁻² M.

3.4. Weight loss

3.4.1. Study the Effect of inhibitor concentrations and temperature on the corrosion rate

The corrosion rate values of carbon steel in absence and presence of different concentrations of the inhibitor in both (0.5 M HCl and 0.5 M H₂SO₄) at various temperatures are listed in Table (3). The data listed in Table (3) showed that the corrosion rate values decreased as the concentrations of the inhibitor increased, i.e. the corrosion inhibition efficiency increased with increasing the inhibitor

concentration. This behavior was due to the adsorption and the coverage of inhibitor on carbon steel surface. Also, the data in Table (3) showed that the corrosion rate of carbon steel increased with increasing temperature for both uninhibited and inhibited solutions. The corrosion rate of the carbon steel increased more rapidly with temperature increasing in the absence and presence of the inhibitor. These results confirmed that the synthesized inhibitor acted as well an efficient inhibitor in the range of the temperatures studied (25_55 °C).

Table 3 Weight loss data for carbon steel in both (0.5 M HCl and H₂SO₄) without and with different concentrations of the synthesized Schiff base at various temperatures

Acid name	Inhibitor conc.(M)	25 °C		
		K (mgcm ⁻² h ⁻¹)	θ	η_w (%)
H ₂ SO ₄ (0.5M)	0	1.094714506	–	–
	1×10 ⁻³	0.345968364	0.683964758	68.39647577
	2.5×10 ⁻³	0.288387346	0.736563877	73.65638767
	5×10 ⁻³	0.232349537	0.787753304	78.7753304
	7.5×10 ⁻³	0.182388117	0.83339207	83.33920705
	1×10 ⁻²	0.130979938	0.880352423	88.03524229
HCl (0.5M)	0	0.633101852	–	–
	1×10 ⁻³	0.179108796	0.717093236	71.70932358
	2.5×10 ⁻³	0.124807099	0.802864107	80.28641073
	5×10 ⁻³	0.082658179	0.869439366	86.94393662
	7.5×10 ⁻³	0.060378086	0.904631322	90.46313224
	1×10 ⁻²	0.038387346	0.93936624	93.93662401
Acid name	Inhibitor conc.(M)	35 °C		
		k (mgcm ⁻² h ⁻¹)	θ	η_w (%)
H ₂ SO ₄ (0.5M)	0	1.866608796	–	–
	1×10 ⁻³	0.722222222	0.613083243	61.30832429
	2.5×10 ⁻³	0.630594136	0.66217124	66.21712396
	5×10 ⁻³	0.517939815	0.72252364	72.25236397
	7.5×10 ⁻³	0.40788966	0.781480907	78.14809074
	1×10 ⁻²	0.323591821	0.826641864	82.66418643
HCl (0.5M)	0	0.94376929	–	–
	1×10 ⁻³	0.321180556	0.659683189	65.96831886
	2.5×10 ⁻³	0.236496914	0.749412366	74.94123659
	5×10 ⁻³	0.174864969	0.814716403	81.47164027
	7.5×10 ⁻³	0.127218364	0.86520184	86.52018396
	1×10 ⁻²	0.091049383	0.903525805	90.35258048

Acid name	Inhibitor conc.(M)	45 °C		
		k (mgcm ⁻² h ⁻¹)	θ	η_w (%)
H ₂ SO ₄ (0.5M)	0	3.149594907	–	–
	1×10 ⁻³	1.384645062	0.560373603	56.03736028
	2.5×10 ⁻³	1.257040895	0.600888072	60.08880723
	5×10 ⁻³	1.08130787	0.656683509	65.66835094
	7.5×10 ⁻³	0.878761574	0.720992191	72.09921911
	1×10 ⁻²	0.716338735	0.772561629	77.25616292
HCl (0.5M)	0	1.352141204	–	–
	1×10 ⁻³	0.561053241	0.585063129	58.50631286
	2.5×10 ⁻³	0.450424383	0.666880662	66.6880662
	5×10 ⁻³	0.315393519	0.766745132	76.67451316
	7.5×10 ⁻³	0.280767747	0.792353235	79.23532349
	1×10 ⁻²	0.193383488	0.856979813	85.69798131
Acid name	Inhibitor conc.(M)	55 °C		
		K (mgcm ⁻² h ⁻¹)	θ	η_w (%)
H ₂ SO ₄ (0.5M)	0	4.455343364	–	–
	1×10 ⁻³	2.213445216	0.503193124	50.31931245
	2.5×10 ⁻³	2.085262346	0.531963717	53.19637174
	5×10 ⁻³	1.813078704	0.593055225	59.30552248
	7.5×10 ⁻³	1.541570216	0.653995194	65.39951941
	1×10 ⁻²	1.244502315	0.720671963	72.06719633
HCl (0.5M)	0	1.823591821	–	–
	1×10 ⁻³	0.881847994	0.516422489	51.6422489
	2.5×10 ⁻³	0.681905864	0.626064421	62.60644206
	5×10 ⁻³	0.565200617	0.690061882	69.00618818
	7.5×10 ⁻³	0.460551698	0.747448035	74.74480351
	1×10 ⁻²	0.331693673	0.818109695	81.81096948

3.4.2. Study

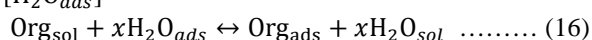
the Effect of inhibitor concentrations and temperatures on corrosion inhibition efficiency.

The values of inhibition efficiencies for carbon steel in both (0.5 M HCl and 0.5 M H₂SO₄) in the absence and presence of different concentrations of the synthesized inhibitor at various temperatures are listed in Table (3). The results listed in Table (3) showed that inhibition efficiency (η_w) increased as the concentration of inhibitor increasing. The maximum corrosion inhibition efficiency for the inhibitor was obtained at 1×10⁻² M. The obtained weight loss results

were in a good agreement with those obtained from EIS and potentiodynamic polarization measurements.

3.5. Adsorption isotherm

The adsorption of organic inhibitor molecule from the aqueous solution could be regarded as a quasi-substitution process between the organic compound in the aqueous phase [Org_{sol}] and water molecule at the electrode surface [H₂O_{ads}]



Evaluating Synthesized Schiff base as Corrosion Inhibitor on Carbon Steel in 0.5 M HCl and 0.5 M H₂SO₄

Where x is the size ratio, that is, the number of water molecule replaced by one organic inhibitor. In this situation, the adsorption of the synthesized inhibitor was accompanied by desorption of water molecule from the surface. Plots of C/θ vs. C (Langmuir's adsorption plots) yielded straight lines. The intercept of each straight line was equal to the

reciprocal of the binding constant Figs.6 (a, b). Values of the binding constant are listed in Table (4). The higher values of the binding constant indicated higher adsorption of the synthesized inhibitor on the carbon steel surface in both of 0.5 M HCl and 0.5 M H₂SO₄ solutions.

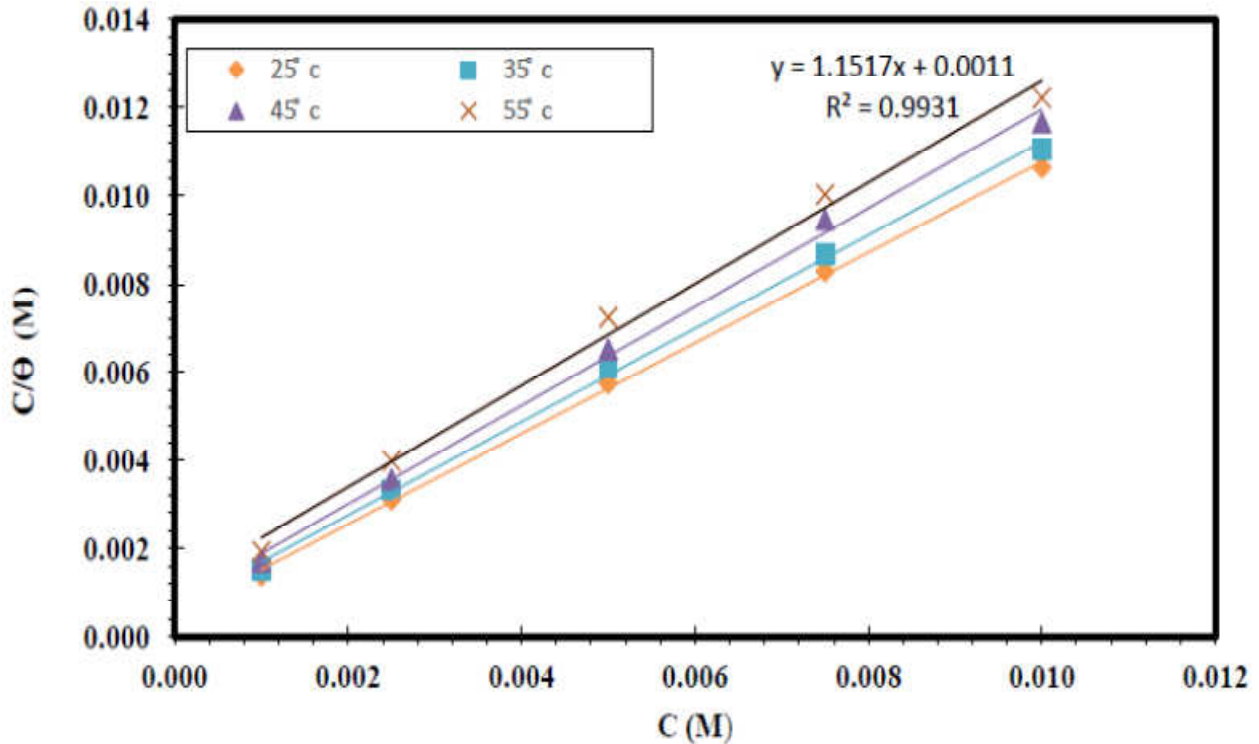


Fig .6a Langmuir's adsorption plots for carbon steel in 0.5 M HCl containing different concentrations of S.B at various temperatures.

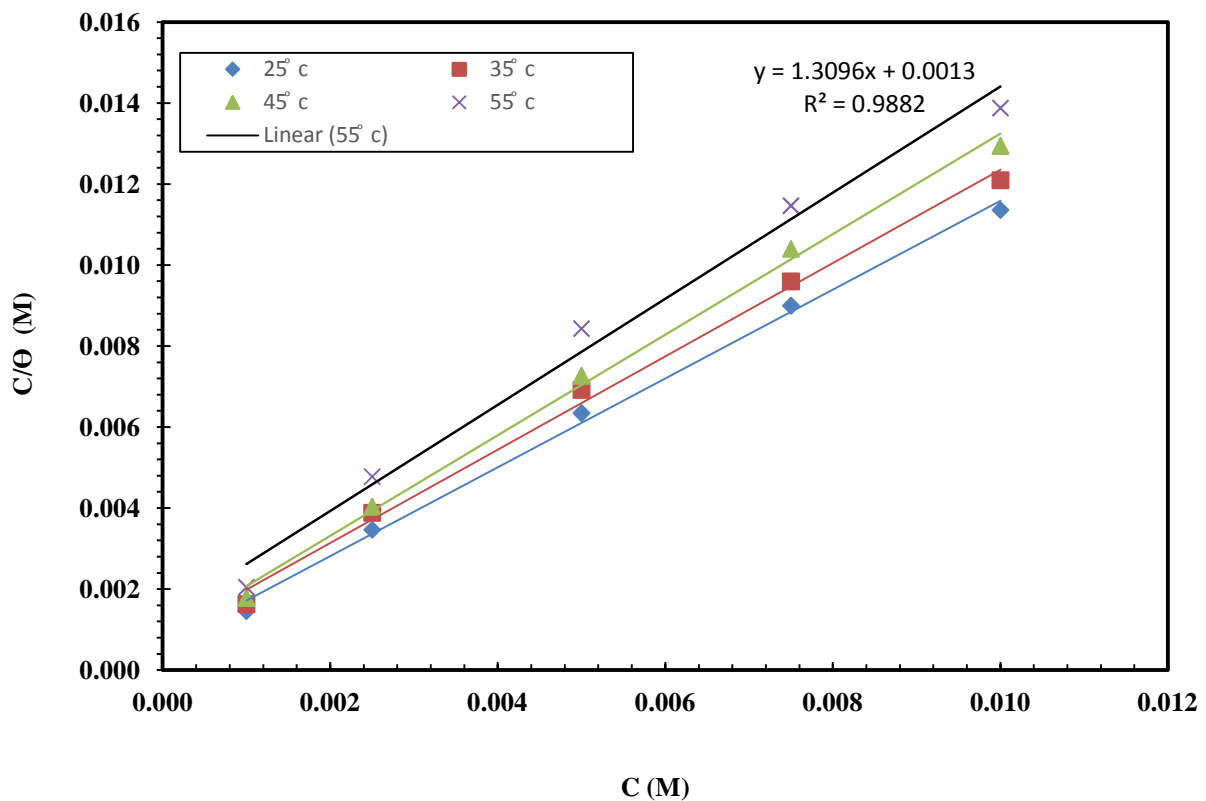


Fig.6 b Langmuir's adsorption plots for carbon steel in 0.5 M H₂SO₄ containing different concentrations of S.B at various temperatures.

Table 4. Standard thermodynamic parameters of adsorption on carbon steel surface in both (0.5 M HCl and 0.5 M H₂SO₄) containing different concentrations of the synthesized Schiff base.

Acid name	Temperature (°C)	K _{ads} (M ⁻¹)	ΔG _{ads} (KJ mol ⁻¹)	ΔH _{ads} (KJ mol ⁻¹)	ΔS _{ads} (J mol ⁻¹ K ⁻¹)
HCl (0.5M)	25	111583.766	-28.7957	-21.6215701	24.07411711
	35	87183.4325	-29.1301		24.37824548
	45	65342.8874	-29.3135		24.18831697
	55	50564.5704	-29.5361		24.12956631
H ₂ SO ₄ (0.5M)	25	93969.188	-28.239	-19.70147	28.6495
	35	70827.7582	-28.598		28.88499
	45	57749.2285	-28.9868		29.19927
	55	44837.8977	-29.2083		28.98421

3.6. Standard thermodynamic adsorption parameters

Generally, values of ΔG_{ads}° up to $(-20 \text{ kJ mol}^{-1})$ were consistent with the electrostatic interaction between the charged molecules and the charged metal physical adsorption. On the other hand, negative values less than $(-40 \text{ kJ mol}^{-1})$ involved sharing or transferring of electrons from the inhibitor molecule to the metal surface to form a coordinate type of bond (chemisorption)²⁷. The calculated ΔG_{ads}° values in Table (4) are ranging between -28.79 to $-29.53 \text{ kJ mol}^{-1}$ in 0.5 HCl and -28.23 to $-29.21 \text{ kJ mol}^{-1}$. This indicated that both physical and chemical adsorptions took place²⁸. Results listed in Table (4) showed that ΔG_{ads}° values decreased with increasing the temperature in both of 0.5 M HCl and 0.5 M H₂SO₄ indicating that the adsorption of inhibitor is more spontaneously with increasing temperature. To obtain the standard enthalpy, plotting $\ln K_{ads}$ vs. $1/T$ yielded straight line according to Eq. (11) with slope equal $-\Delta H_{ads}^{\circ}/R$. The negative sign of ΔH_{ads}° values Table(4) of the synthesized inhibitor (Schiff base) indicated that the adsorption of inhibitor molecule was an exothermic process²⁹. In an exothermic process, chemisorption is distinguished from physisorption by considering the absolute value of $-\Delta H_{ads}^{\circ}$. For the chemisorption process, it approaches $(100 \text{ kJ mol}^{-1})$; while for the physisorption process, it is less than (40 kJ mol^{-1}) . In this study, the $-\Delta H_{ads}^{\circ}$ values are around $(-19.70$ to $-21.62 \text{ kJ mol}^{-1})$ indicated that only physical adsorption took place. The obtained ΔS_{ads}° values were listed in Table (4). The positive values of ΔS_{ads}° mean that the adsorption process is accompanied by an increase in entropy, which is the driving force for the adsorption of inhibitor onto the carbon steel surface

3.7. Activation parameters

The Arrhenius plots of $\ln k$ vs. $1/T$ for the blank and different concentrations of the synthesized Schiff base were shown in Figs 7 (a, b). The obtained activation parameter depicted in Table 5 showed that all the linear regression coefficients (r^2) (0.965 to 0.978) in 0.5 M HCl and (0.995 to 0.998) in 0.5 M H₂SO₄ are very close to 1, that means the linear relationship between $\ln k$ and $1/T$ is good. The value of E_a in the presence of synthesized inhibitor Schiff base is higher than that in the uninhibited acid solutions. Many studies³⁰ showed that E_a increased in the presence of inhibitor than in the absence of inhibitor. Eq. (13) showed that, $-E_a/R$ is the slope of the straight line ($\ln k$ vs. $1/T$), so

the value of E_a could elucidated the effect of temperature on corrosion inhibition. The relationships between the temperature dependence of percentage η_w of the inhibitor and the E_a can be classified according to temperature effects²³ as follows: (i) η_w decreases with increase in temperature, E_a (inhibited solution) $>$ E_a (uninhibited solution), (ii) η_w increases with increase in temperature, E_a (inhibited solution) $<$ E_a (uninhibited solution), and (iii) η_w does not change with temperature, E_a (inhibited solution) = E_a (uninhibited solution). In the present work E_a values in Table 5 indicated that E_a (inhibited solution) $>$ E_a (uninhibited solution), and E_a increased with increasing in the inhibitor concentrations in 0.5 M HCl and 0.5 M H₂SO₄. This is further confirmation that η_w values decreased with increasing temperature. This behavior is indicated that the adsorption of the inhibitor schiff base on the carbon steel in 0.5 M HCl and 0.5 M H₂SO₄ is physical adsorption. Plotting of $\ln(K/T)$ against $1/T$, Eq. (14), for carbon steel dissolution in 0.5 M HCl and 0.5 M H₂SO₄ in the absence and presence of different concentrations from the synthesized inhibitor, gave straight lines as shown in Fig. 8(a, b). Data in Table 5 represented the values of (ΔH^* and ΔS^*), which were calculated from the slope of $-\Delta H^*/R$ and the intercept of $(\ln(R/N_A h) + \Delta S^*/R)$ of the straight lines. Values of ΔH^* and ΔS^* were calculated and listed in Table 5. Inspection of these data revealed that the activation parameters (ΔH^* and ΔS^*) of the dissolution reaction of carbon steel in 0.5 M HCl and 0.5 M H₂SO₄ in the presence of the inhibitor were more than those in the absence of inhibitor (blank). The positive signs of the enthalpy (ΔH^*) reflected the endothermic nature of the steel dissolution process and indicated that the dissolution of carbon steel was difficult³⁰. The entropy of activation in presence and absence of the inhibitor was large and negative. This implies that the activated complex in the rate determining step represents association rather than dissociation, indicating that a decrease in disorder takes place, going from reactant to the activated complex.

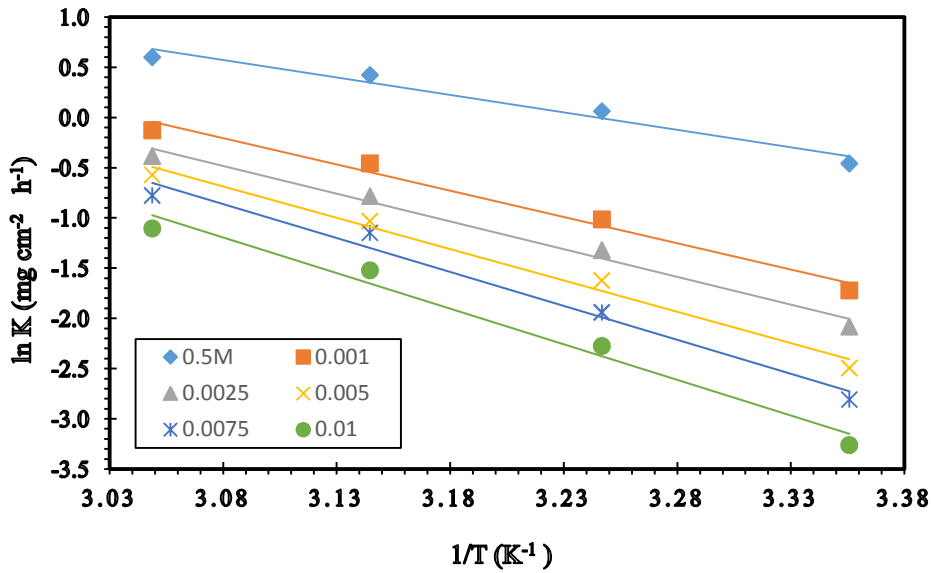


Fig.7a Arrhenius plots related to the corrosion rate of CS in 0.5 M HCl in absence and presence of different concentrations of S.B at various temperatures.

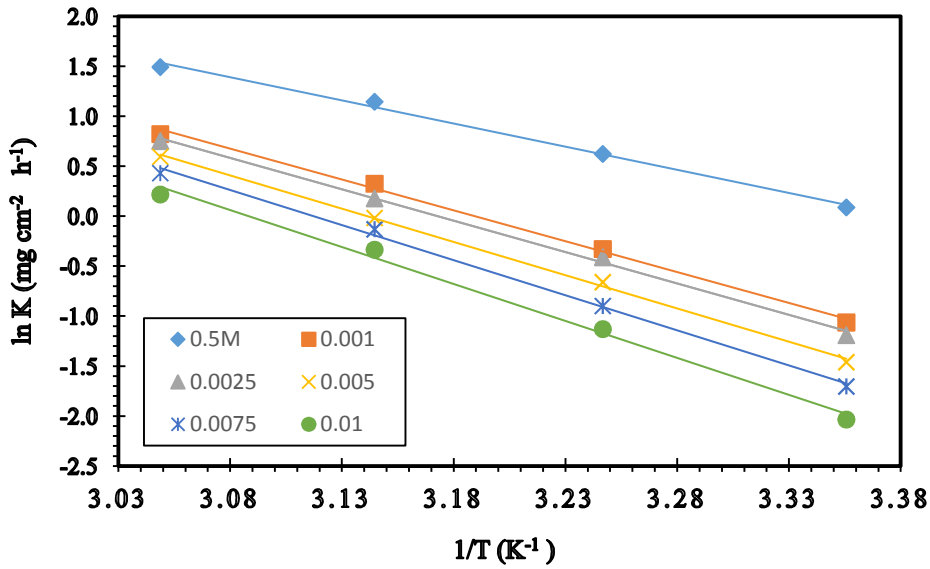


Fig.7b Arrhenius plots related to the corrosion rate of CS in 0.5 M H₂SO₄ in absence and presence of different concentrations of S.B at various temperatures.

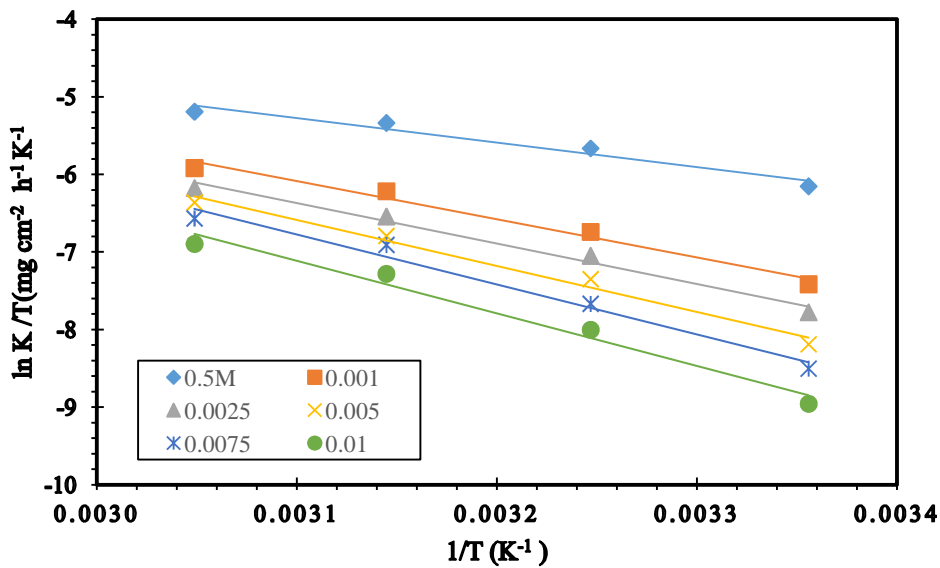


Fig.8a Arrhenius plots of ln (k/T) vs. 1/T related to the corrosion rate of CS in 0.5 M HCl in absence and presence of different concentrations of S.B at various temperatures

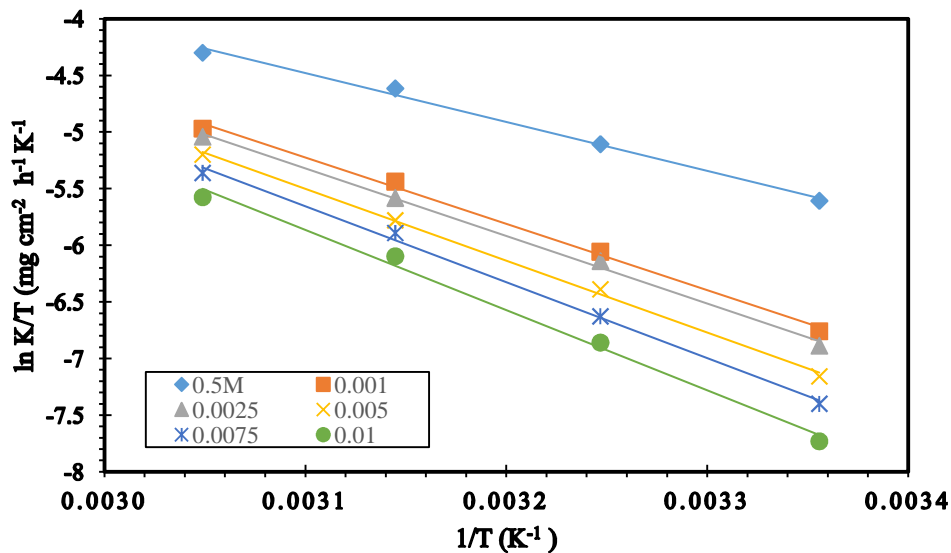


Fig.8 Arrhenius plots of $\ln(k/T)$ vs. $1/T$ related to the corrosion rate of CS in 0.5 M H_2SO_4 in absence and presence of different concentrations of S.B at various temperatures

Table 5. Activation parameters values for carbon steel in both (0.5 M HCl and 0.5 H_2SO_4) in the absence and presence of different concentrations of the synthesized Schiff base.

Acid name	Conc of inhibitor (M)	E_a (KJ mol ⁻¹)	ΔH^* (KJ mol ⁻¹)	ΔS^* (J mol ⁻¹ K ⁻¹)
HCl (0.5M)	Blank	41.7742945	38.0163514	-601.443
	1×10 ⁻³	63.0232386	59.2652954	-545.335
	2.5×10 ⁻³	66.4528544	62.6949112	-538.123
	5×10 ⁻³	75.00336	71.2454168	-514.234
	7.5×10 ⁻³	81.2881521	77.5302089	-496.996
	1×10 ⁻²	85.2896002	81.531657	-488.671
H_2SO_4 (0.5M)	Blank	55.7603187	52.0023755	-548.514
	1×10 ⁻³	74.2603235	70.5023803	-500.143
	2.5×10 ⁻³	75.5508225	71.7928794	-497.291
	5×10 ⁻³	80.100222	76.3422789	-485.37
	7.5×10 ⁻³	84.4331241	80.675181	-473.783
	1×10 ⁻²	88.9594689	85.2015258	-462.253

3.8. Mechanism of inhibition

The adsorption of organic molecule on the solid surfaces cannot be considered only as purely physical or as purely chemical adsorption phenomenon. In physical adsorption, the inhibitor molecule can be adsorbed on the carbon steel surface via electrostatic interaction between the charged metal surface and charged inhibitor molecule. While in the chemical adsorption of the studied Schiff base arises from the donor acceptor interactions between free electron pairs of the hetero atoms and π -electrons of multiple bonds as well as phenyl group and vacant d-orbitals of iron³¹. It has been reported that the adsorption of heterocyclic compounds occurs with the aromatic rings sometimes parallel but mostly normal to the metal surface. The orientation of molecule could be dependent on the pH and/or electrode potential. However, more work should be provided to confirm the above arguments³². In the case of parallel adsorption of inhibitor molecule, the steric factors also must be taken into consideration. The free energy values of adsorption were lesser than (-40 kJ mol⁻¹) indicating the physical adsorption of the synthesized Schiff base. Schiff base have basic character and expected to be protonated in

equilibrium with the corresponding neutral form in strong acid solutions. It is also well known that carbon steel surface in (0.5 M HCl and 0.5 M H_2SO_4) charges negative charge because of $E_{corr} - E_{q=0}$ (zero charge potential) < 0, thus, it is easily for the positively charged inhibitor to approach the negatively charged carbon steel surface due to the electrostatic attraction. Finally, it should also be emphasized that, the large size and high molecular weight of Schiff base molecule can also contribute the greater inhibition efficiency of the studied Schiff base as inhibitor. The differences in the corrosion inhibition efficiency of Schiff base inhibitor in different concentrations and temperatures can be attributed to the molecular structure effect. In addition, due to the rigidity of the π -system of the inhibitor because of the coordination through the lone pairs on the nitrogen atoms of ((-C=N- and hetero rings) with the partially filled d-orbitals of metal surface which facilitate the delocalization of the electrons of π -system and producing coordination bonds which were expected to produce different adsorption centers (Chemisorption) and hence corrosion inhibition efficiency.

3.9. Morphological examination

The (SEM) image of the surface of the carbon steel specimens explained how much changes happen before and after protection of inhibitor from corrosive media (0.5M hydrochloric acid, 0.5M sulfuric acid) for 24hr shown in Fig. (9). The results of SEM micrograph image illustrate inhibition efficiency of Schiff base for the surface of carbon steel specimens in absence and presence of inhibitor in (0.5M hydrochloric acid) shown in Fig. (9), while another specimen with the same conditions and time but added (0.5M sulfuric acid) the result shown in Fig. (9). The difference is obvious with the Schiff base inhibitor which reveals that Schiff base adsorbed at the surface of carbon steel form a protection layer against corrosive solutions this is good evidence of high inhibition efficiency of corrosion inhibitor.

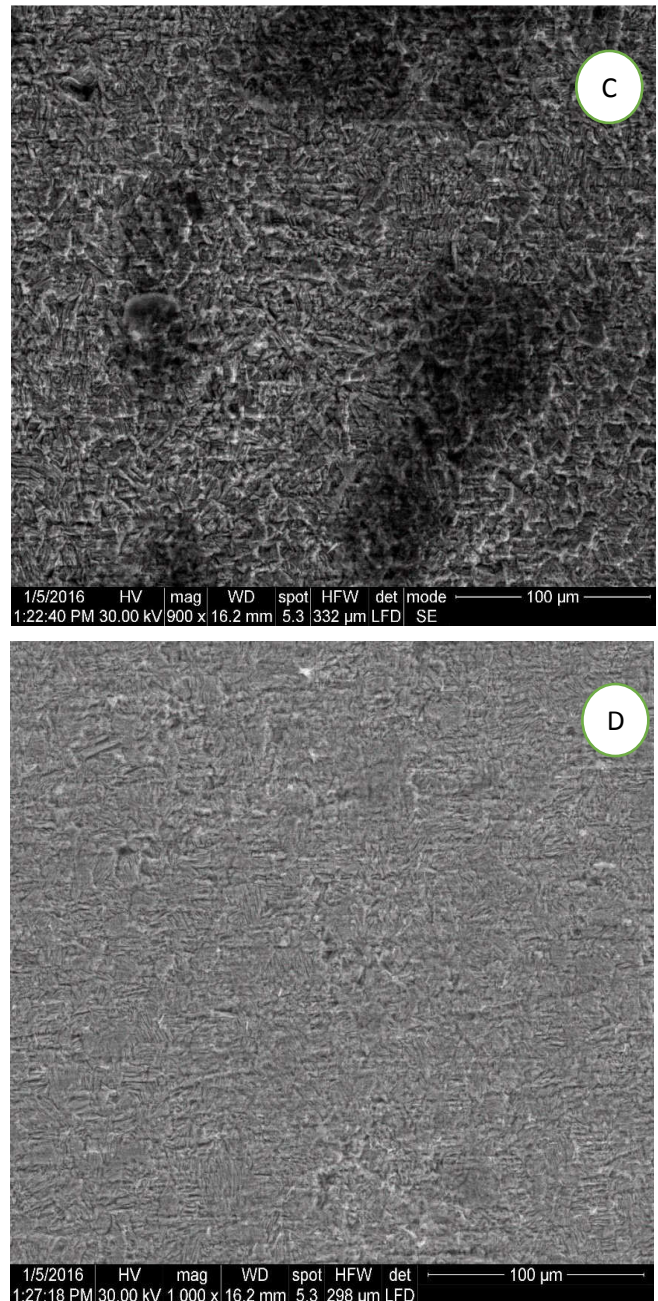
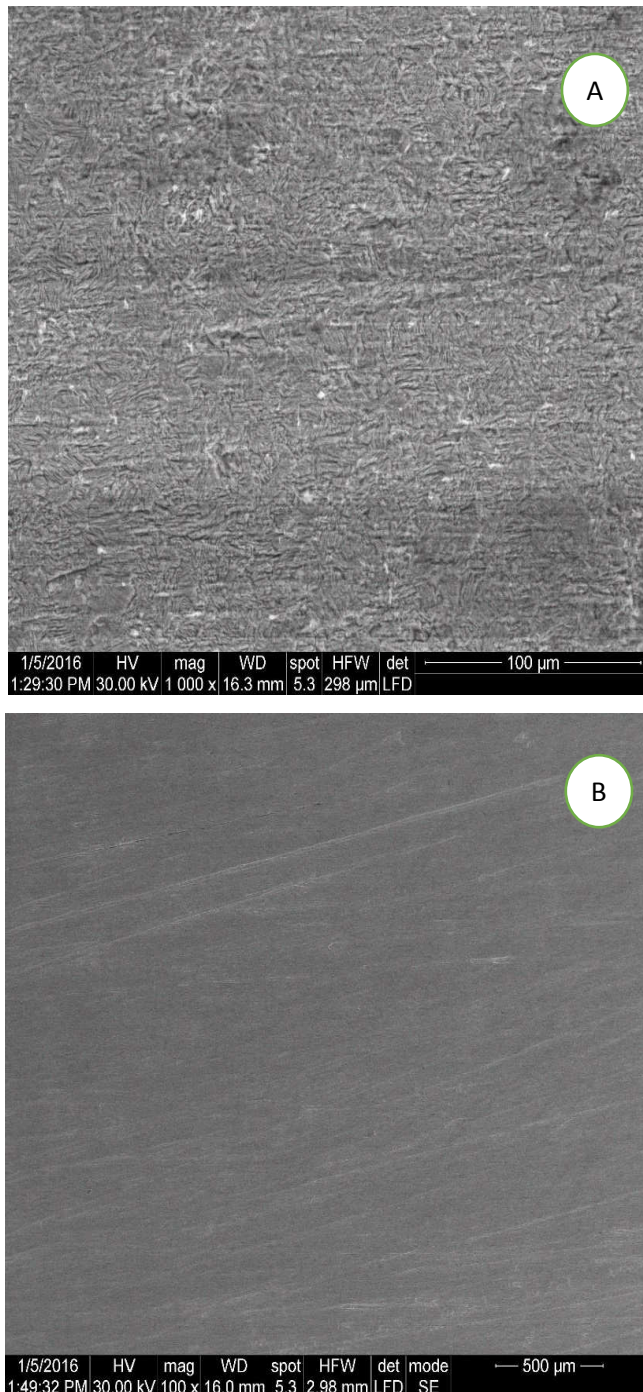


Fig. 9. The SEM images of carbon steel surface after 24 h immersion period, (A) 0.5 M HCl, (B) 0.5 M HCl + 1×10^{-2} M of inhibitor, (C) 0.5 M H₂SO₄, and (D) 0.5 M H₂SO₄ + 1×10^{-2} M of inhibitor.

IV. CONCLUSIONS

- (1) The prepared Schiff base is excellent inhibitors show remarkable result with both corrosive media (hydrochloric acid, sulfuric acid) to carbon steel the efficiency reach to (93.93 %), there is a prosperity relation with the inhibitor concentration, opposite relation with temperature.
- (2) Inhibition efficiency was specify by three different method: weight loss, potentiodynamic polarization, electrochemical impedance method all giving a hassling result.
- (3) The thermodynamic parameters describes the adsorption of Schiff Base on the surface of carbon steel according to the value of Gibbs free energy obeys Langmuir isotherm and Mixed physical, chemical

adsorption. The heat of adsorption is exothermic according to enthalpy, the entropy show disorder due to start adsorption of inhibitor on the carbon steel surface in both corrosive media.

- (4) Not only the values of activation energy (E_a) increased after adding the Schiff base but also the double layer capacitance obtained from the EIS.
- (5) The (SEM) show that Schiff base makes a thin layer of organic molecules at the surface of Carbon steel regard as a good protection against (Hydrochloric acid, sulfuric acid) which approved the Schiff base is a good inhibitor for carbon steel.

REFERENCE

1. M. ElAzhar, B. Mernari, M. Traisnel, F. Bentiss, M. Lagrene´ e, Corrosion inhibition of mild steel by the new class of inhibitors [2,5-bis(*n*-pyridyl)-1,3,4-thiadiazoles] in acidic media , 2001,Corrosion Sci.,vol 43, 2229.
2. H. Derya Lece, Kaan C. Emregul, Orhan Atakol, Inhibitive Effect of N, N-bis (2-chloroethylaminobenzaldehyde) Ethylthiosemicarbazone on the Corrosion of Mild Steel in 1N H₂SO₄, 2008Corr. Sci. , 50 1460–1468.
3. H. Shokry, M. Yuasa, I. Sekine, R.M. Issa, H.Y. El-Baradie, G.K. Gomma, Corrosion inhibition of mild steel by Schiff base compounds in various aqueous solutions Corros.Sci, 1998, 40, 2173–2186.
4. M. Lashgari, M.-R. Arshadi, S. Miandari, The enhancing power of iodide on corrosion prevention of mild steel in the presence of a synthetic-soluble Schiff-base: Electrochemical and surface analyses, Electrochimica , 2010 , Acta 55 6058–6063.
5. S. Bilgic, N. Caliskan, J. Appl, Corrosion Inhibition Properties of orepinephrine Molecules on Mild Steel in Acidic Media Electrochimica, 2001, 31, 79–83.
6. Labena A, Hegazy MA, Horn H, Müller E, The biocidal effect of a novel synthesized gemini surfactant on environmental sulfidogenic bacteria: planktonic cells and biofilms. Mater Sci Eng, 2015, 47,367–375.
7. M.A. Hegazy, A.S. El-Tabei, A.H. Bedair, M.A. Sadeq, An investigation of three novel nonionic surfactants as corrosion inhibitor for carbon steel in 0.5 MH₂SO₄, Corros. Sci, 2012 54, 219–230.
8. M.A. Hegazy, M.F. Zaky, Inhibition effect of novel nonionic surfactants on the corrosion of carbon steel in acidic medium, Corros. Sci., 2010, 52, 1333–1341.
9. M.A. Migahed, A.M. Abdul-Raheim, A.M. Atta, W. Brostow, Synthesis and evaluation of a new water soluble corrosion inhibitor from recycled poly(ethylene terphthalate),Mater. Chem. Phys., 2010,121, 208–214.
10. E.E. Oguzie, Y. Li, F.H. Wang, Effect of 2-amino-3-mercaptopropanoic acid (cysteine) on the corrosion behaviour of low carbon steel in sulphuric acid Electrochim.,2007, Acta 53 ,909–914.
11. M.A. Hegazy, M. Abdallah, H. Ahmed, Novel cationic gemini surfactants as corrosion inhibitors for carbon steel pipelines Corros. Sci., 2010, 52, 2897–2904.
12. S. Ghareba, S. Omanovic, and Interaction of 12-aminododecanoic acid with a carbon steel surface: Towards the development of ‘green’ corrosion inhibitors Corros. Sci., 2010, 52, 2104–2113.
13. A.Y. El-Etre, J. Inhibition of acid corrosion of carbon steel using aqueous extract of olive leaves, Colloid Interface Sci., 2007, 314, 578–583.
14. G.Quartarone,M. Battilana, L. Bonaldo, T. Tortato, Investigation of the inhibition effect of indole-3-carboxylic acid on the copper corrosion in 0.5 M H₂SO₄, 2008,Corros. Sci. 50, 3467–3474.
15. Eugenio A,Flores, Octavio Olivares, Natalya V. Likhanova, Marco .Dominguez-Aguilar, Noel Nava, Diego Guzman-Lucero, Monica Corrales, Sodiumphalamates as corrosion inhibitors for carbon steel in aqueous hydrochloric acid solution Corros. Sci., 2011, 53, 3899–3913.
16. S.K. Shukla, M.A. Quraishi, 4-Substituted anilinomethylpropionate: New and efficient corrosion inhibitors for mild steel in hydrochloric acid solution Corros. Sci. 51 (2009) 1990–1997.
17. N. Putilova, S. Balezin, V. Barannik, Metallic Corrosion Inhibitors, Pergamon Press, Oxford, UK, 1960.
18. M. A. Hegazy Eid M. S. Azzam Nadia G. Kandil A. M. Badawi R. M. Sami Corrosion Inhibition of Carbon Steel Pipelines by Some New Amphoteric and Di-cationic Surfactants in Acidic solution by Chemical and Electrochemical Methods , Journal of Surfactants and Detergents,2016,19,864-866.
19. H.H. Hassan, E. Abdelghani, M.A. M.A. Amin,Inhibition of mild steel corrosion in hydrochloric acid solution by triazole derivatives: Part I. Polarization and EIS studies , Electrochim. Acta, 2007, 52, 6359–6366.
20. A.M. Abdel-Gabar, B.A. Abd-El-Nabey, I.M. Sidahmed, A.M. El-Zayady, M.Saadawy, Inhibitive action of some plant extracts on the corrosion of steel in acidic media Corros. Sci., 2006, 48, 2765–2779.
21. K.F. Khaled, Molecular simulation, quantum chemical calculations and electrochemical studies for inhibition of mild steel by triazoles, Electrochim. Acta, 2008, 53, 3484–3492.
22. S.V. Lamaka, M.L. Zheludkevich, K.A. Yasakau, R. Serra, S.K. Poznyak, M.G.S.Ferreira, Nanoporous titania interlayer as reservoir of corrosion inhibitors for coatings with self-healing ability Prog. Org. Coat., 2007, 58, 127–135.
23. H. Duan, K. Du, C. Yan, F. Wang, Electrochemical corrosion behavior of composite coatings of sealed MAO film on magnesium alloy AZ91D,Electrochim. Acta, 2006, 51, 2898–2908.
24. M. Mahdavian, S. Ashhari, Corrosion inhibition performance of 2-mercaptobenzimidazole and 2-mercaptobenzoxazole compounds for protection of mild steel in hydrochloric acid solution, Electrochim. Acta, 2010, 55, 1720–1724.
25. N.A. Negm, M.F. Zaki, Corrosion inhibition efficiency of nonionic Schiff base amphiphiles of p-aminobenzoic acid for aluminum in 4N HCl , J. Colloid Surf. A: Physicochem. Eng. Aspec. , 2008, 322, 97–102.
26. F. Bentiss, M. Lebrini, M. Lagrenee, Thermodynamic characterization of metal dissolution and inhibitor adsorption processes in mild steel/2,5-bis(*n*-thienyl)-1,3,4-thiadiazoles/hydrochloric acid system, Corros. Sci., 2005, 47, 2915–2931
27. E.A. Noor, A.H. Al-Moubaraki, Mater., Thermodynamic study of metal corrosion and inhibitor adsorption processes in mild steel/1-methyl-4[4 (-X)-styryl pyridinium iodides/hydrochloric acid systems , Chem. Phys.,2008, 110 , 145–154.
28. A.M. Badawi, M.A. Hegazy, A.A. El-Sawy, H.M. Ahmed, W.M. Kamel, Mater., Novel quaternary ammonium hydroxide cationic surfactants as corrosion inhibitors for carbon steel and as biocides for sulfate reducing bacteria (SRB) ,Chem. Phys.,2010,124 , 458–465.
29. M.S. Morad, A.M. Kamal El-Dean, 2, 2'-Dithiobis (3-cyano-4, 6-dimethylpyridine): A new class of acid corrosion inhibitors for mild steel ,Corros. Sci., 2006, 48, 3398–3412.
30. K.P.V. Kumar, M. Sankara Narayana Pillai, G. Rexin Thusnavis, J. Mater., Seed Extract of *Psidium guajava* as Ecofriendly Corrosion Inhibitor for Carbon Steel in Hydrochloric Acid Medium, Sci.Technol.,2011, 27, 12,2011, 1143–1149.
31. M. Behpour, S.M. Ghoreishi, M. Salavati-Niasari, B. Ebrahimi, Mater., Evaluating two new synthesized S–N Schiff bases on the corrosion of copper in 15% hydrochloric acid, Chem.Phys. , 2008,107, 153–157.
32. Lj. Vracar, D.M. Drazic, Adsorption and corrosion inhibitive properties of some organic molecules on iron electrode in sulfuric acid, Corros. Sci., 2002, 44, 1669–1680.